

ELECTRON-ION RECOMBINATION RATE COEFFICIENTS FOR Si I, Si II, S II, S III, C II, AND C-LIKE IONS  
C I, N II, O III, F IV, Ne V, Na VI, Mg VII, Al VIII, Si IX, AND S XI

SULTANA N. NAHAR

Department of Astronomy, Ohio State University, Columbus, OH 43210

*Received 1994 October 3; accepted 1994 November 10*

## ABSTRACT

A new unified treatment for electron-ion recombination is employed to obtain recombination rate coefficients for silicon, sulfur, and carbon ions of importance in the study of the interstellar medium and H II regions in general. Improved and extended results are also presented for ions in the carbon isoelectronic sequence. Recombination rate coefficients are tabulated at a wide range of temperatures, from  $10^1$  to  $10^9$  K. These rates correspond to total electron-ion recombination incorporating both the radiative and dielectronic recombination processes calculated in an ab initio manner.

*Subject headings:* atomic data — atomic processes

## 1. INTRODUCTION

In earlier works (Nahar & Pradhan 1994, 1995, hereafter NP1, NP2), we have presented a unified treatment of electron-ion recombination that incorporates both the radiative recombination (RR) and the dielectronic recombination (DR) processes, which have heretofore been calculated separately in different approximations. The new method enables the calculation of a single, total recombination rate coefficient that may be employed for a variety of astrophysical applications, in particular calculations involving ionization balance in H II regions, the interstellar medium (ISM), active galactic nuclei, and other sources.

We consider all final recombined states of the electron+ion system that couple to the ground state of the recombining ion. These states are divided into two groups: (a) low- $n$  states  $n \leq n_0$  ( $n_0 \approx 10$ ) and (b) the high- $n$  states  $n_0 < n \leq \infty$ . Recombination to low-lying bound states, corresponding to a low principal quantum number  $n$ , is treated as the detailed-balance inverse of photoionization from a given state by virtue of the Milne relation. Partial photoionization cross sections for leaving the ion in the ground state are calculated for all bound states that we designate as “low- $n$ ” states using methods developed for the Opacity Project (Seaton 1987). The ab initio photoionization calculations employ the close coupling approximation and the  $R$ -matrix method (Berrington et al. 1987). Resonances in the photoionization cross sections are resolved in detail. Recombination cross sections and rate coefficients so obtained subsume both the RR and the DR processes for recombination to low- $n$  bound states of the electron+ion system. However, recombination to bound states belonging to “high- $n$ ” complexes is dominated by the DR process over the “background” RR process throughout most of the temperature range. We therefore calculate the DR collision strengths, for recombination via the high- $n$  ( $10 < n \leq \infty$ ) autoionizing resonances in the electron+ion system. The method is based on the precise theory of DR developed by Bell & Seaton (1985) and applied by Pradhan & Seaton (1985) for radiation damping in electron scattering with positive ions. The method devel-

oped for electron+ion recombination thus forms an extension of the close-coupling approximation for photoionization and electron-ion scattering.

Because the calculations are rather extensive, a few ions of astrophysical importance are treated first. In NP2 we applied the new method to selected sulfur and silicon ions abundant in the ISM (Spitzer & Fitzpatrick 1993); results of cross sections and comparison with previous works are given. In the present work total rates and recombination rates for individual states are presented for the S and Si ions and for C II, together with improved results for the C-sequence ions reported earlier in Nahar & Pradhan (1992b, hereafter NP3) with some additional C-like ions. The method involves explicit consideration of a large number of bound states of the recombined electron-ion system, typically a few hundred, and partial recombination rate coefficients into those states are also obtained. The rates for recombination into specific excited states are of interest in recombination-cascade models in general, and spectral formation of recombination lines in particular (Liu et al. 1995). The background nonresonant recombination to the “high- $n$ ” bound states,  $n = 11 - \infty$ , is “topped up” using the hydrogenic approximation; this contribution is small except at the low temperatures as  $T \rightarrow 0$ . Depending on the temperature, the ground state and relatively few of the excited states may dominate the total recombination rate. We tabulate the partial recombination rate coefficients for the low- $n$  states in each ion at a few low temperatures,  $T = 100, 1000, \text{ and } 10,000$  K. For low  $T$  ( $T \leq 10,000$  K) these rates for individual states should represent the total recombination into these states reasonably well.

## 2. COMPUTATIONS

Although the computational details have been explained in NP1 and NP2, a few points may be reemphasized. Present results correspond to newly calculated photoionization cross sections,  $\sigma_{PI}$ , for all the ions. The primary differences between these and earlier results, such as the Opacity Project (OP) photoionization cross sections, are the following: (1) a much larger

eigenfunction expansion is employed in the present work for the target (or the core) ion, and (2) partial photoionization cross sections, with the core ion in the ground state, are employed (rather than the total cross sections as calculated in the OP). As we discussed in NP2, the inclusion of more highly excited target states in the CC expansion allows contributions from the  $\Delta n \neq 0$  states to be added to recombination. This is particularly the case for ions in the carbon isoelectronic sequence, where we have improved the calculations in this manner. The earlier (NP3) eight state close-coupling (CC) calculations, including target states of the  $n = 2$  complex,  $2s^2 2p$  ( $^2P^o$ ),  $2s 2p^2$  ( $^4P$ ,  $^2D$ ,  $^2S$ ,  $^2P$ ),  $2p^3$  ( $^4S^o$ ,  $^2D^o$ ,  $^2P^o$ ), have been extended to 23 states for the present work, including many terms from the  $n = 3$  complex, i.e.,  $2s^2 3s$  ( $^2S$ ),  $2s^2 3p$  ( $^2P^o$ ),  $2s^2 3d$  ( $^2D$ ),  $2s 2p 3s$  ( $^4P^o$ ,  $^2P^o$ ,  $^2P^o$ ),  $2s 2p 3p$  ( $^2P$ ,  $^4D$ ,  $^4S$ ,  $^4P$ ,  $^2D$ ,  $^2S$ ,  $^2D$ ,  $^2P$ ,  $^2S$ ). This increased the number of bound states, resulting in significant enhancement in recombination rates at the high temperatures. The total number of low- $n$  bound states,  $N_{\text{bnd}}$ , in the new calculations for each ion are presented in Table 2; the number of bound states increases with ion charge.

One important feature of the present calculations is that the near-threshold resonances in the photoionization cross sections are resolved with a finer energy mesh than the OP cross sections, and the observed energies for the ion core states are used in the calculations to obtain more accurate resonance positions. For example, photoionization cross sections for silicon ions in the present work are better resolved than in the OP work by Nahar & Pradhan (1992a, 1993). As explained in NP2, it is crucial that the near-threshold resonances are resolved fully for the recombination rate coefficients,  $\alpha_R(T)$ , to minimize the large uncertainties at low temperatures. The importance of this fact may be appreciated from Figure 1, which presents the  $\alpha_R(T)$  values for the recombination process  $e + \text{C III} \rightarrow \text{C II}$ , obtained by employing photoionization cross sections with fine energy resolution up to about 0.4 rydbergs above the first ionization threshold. At low  $T$  the  $\alpha_R(T)$  values from Figure 8 of NP1, using earlier cross sections which did not fully resolve the resonance structures in the low-energy region, are considerably lower than the new  $\alpha_R(T)$  values at low  $T$ . The present total C II recombination rate coefficients are in good agreement with the earlier results for low- $T$  DR rates by Nussbaumer & Storey (1983) and with the high- $T$  DR rates by Jacobs et al. (1978; the values presented here are taken from the fits of their values by Shull & Van Steenberg 1982).

### 3. RESULTS AND DISCUSSIONS

The total recombination rate coefficients,  $\alpha_R(T)$ , of the 15 ions—Si I, Si II, S II, S III, and C II and the carbon like ions C I, N II, O III, F IV, Ne V, Na VI, Mg VII, Al VIII, Si IX, and S XI—are obtained and presented in Table 1 for a wide temperature range from  $10^1$  to  $10^9$  K with a temperature mesh of  $\Delta(\log_{10} T) = 0.1$ .

The general form of the total recombination rate coefficient is found to be as follows. Beginning with a high value, owing to the  $T^{-\gamma}$  ( $\gamma > 0$ ) dependence of  $\alpha_R(T)$  and near-threshold resonances, there is a relatively sharp decrease with temperature in the low- $T$  region. Presence of near-threshold resonances may enhance the rate considerably, as in the case of  $e +$

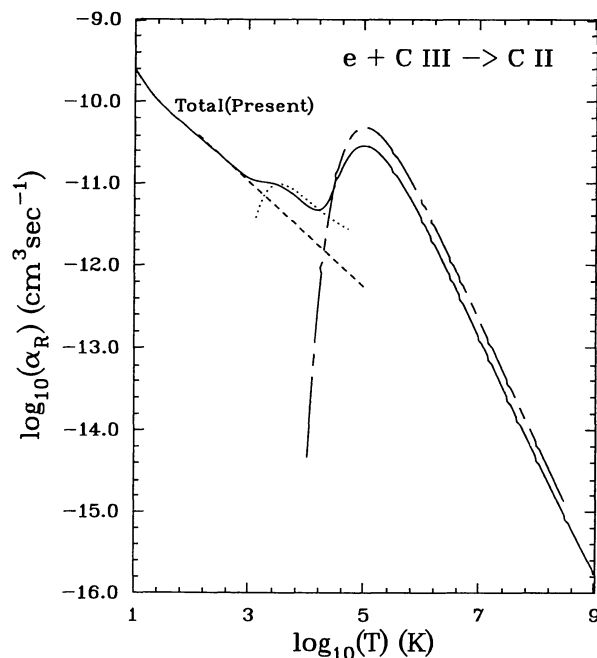


FIG. 1.—Total recombination rate coefficient,  $\alpha_R(T)$  (solid curve), for  $e + \text{C III} \rightarrow \text{C II}$  obtained using photoionization cross sections where the resonances near the ionization threshold are resolved with finer energy mesh (present resolution). Comparison is made with RR rates by Aldrovandi & Péquignot (1973) (dashed curve), low- $T$  DR rates by Nussbaumer & Storey (1983) (dotted curve), and high- $T$  DR rates by Jacobs et al. (1979) (long-dash-short-dash curve). Finer resolution has brought the proper structures in  $\alpha_R(T)$ , agreeing better with earlier calculations.

Mg VII  $\rightarrow$  Mg VII at low temperatures (Fig. 3). The decrease in  $\alpha_R(T)$  may be reversed if the DR type contribution from low-lying autoionizing resonances is appreciable, leading to a low- $T$  bump. At higher temperatures, when DR alone dominates,  $\alpha_R(T)$  exhibits a wider and more pronounced bump. There may also be further small bumps in the high- $T$  region due to additional sets of resonances associated with the  $\Delta n \neq 0$  core transitions. Figure 2 illustrates such features for the recombination of (a)  $e + \text{Mg VIII} \rightarrow \text{Mg VII}$  and (b)  $e + \text{S XII} \rightarrow \text{S XI}$ , and compares the present total recombination rate coefficients,  $\alpha_R(T)$  (solid curve), with previous calculations of RR rates by Aldrovandi & Péquignot (1973) (dashed curve), and high-temperature DR rates by Jacobs et al. (1979) (long-dash-short-dash curve). The first bump in  $\alpha_R(T)$  in the low- $T$  region for Mg VII is due to resonances in the near-threshold region (low- $n$  contribution), while for S XI one sees two bumps in the high- $T$  region, one due to DR contribution from the  $\Delta n = 0$  dipole core transitions and the other from the  $\Delta n \neq 0$  dipole core transitions.

Figure 3 presents the recombination rates for all 10 carbon-like ions: C I, N II, O III, F IV, Ne V, Na VI, Mg VII, Al VIII, Si IX, and S XI. For the C-like ions the present 23 state eigenfunction expansion yields a larger number of electron+ion bound states than the earlier work NP3, and resulted in a significant increase in  $\alpha_R(T)$ . In addition, the present work includes the effect of dipole core transitions with  $\Delta n \neq 0$ . Along the carbon-sequence ions,  $\alpha_R(T)$  generally increases, in the low- $T$  region, with increasing ion charge; although the background photo-





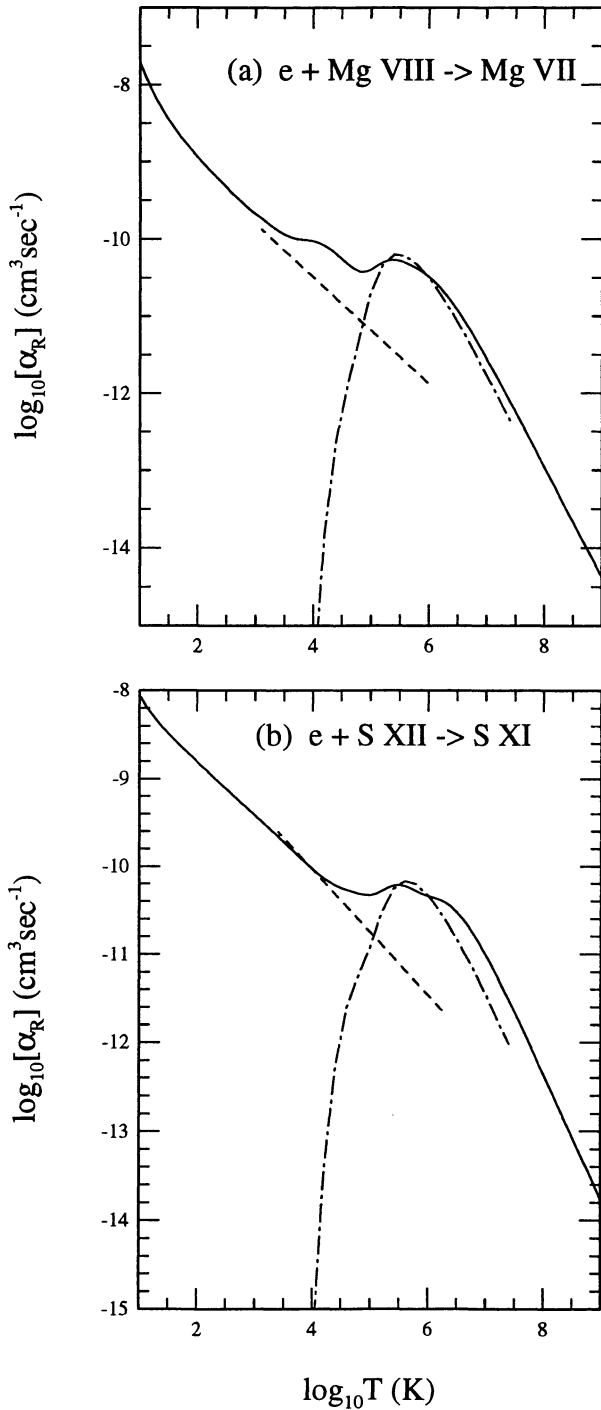


FIG. 2.—Total recombination rate coefficient,  $\alpha_R(T)$  (solid curve), for (a)  $e + \text{Mg VIII} \rightarrow \text{Mg VII}$  and (b)  $e + \text{S XII} \rightarrow \text{S XI}$ . Also shown are RR rates by Aldrovandi & Péquignot (1973) (dashed curve) and high- $T$  DR rates by Jacobs et al. (1979) (dot-dashed curve).

ionization cross sections decrease approximately as  $z^{-2}$ , the number of low- $n$  bound states increases, resulting in higher recombination rates. However, because of the presence of low- $T$  bumps, the rate coefficients sometimes overlap, and there is no systematic pattern. In contrast to the low- $T$  region, the high-

$T$  region (where DR dominates over RR) shows diminishing enhancement in  $\alpha_R(T)$  with ion charge, while the peak value shifts gradually to higher temperatures. Consistent with the estimated uncertainties in close-coupling calculations for photoionization cross sections and excitation collision strengths, the present rates should be accurate to within 10%–20% in most of the temperature region.

The present report also includes recombination rate coefficients for several individual states of the recombined electron+ion system. Table 2 lists the “low- $n$ ” states that dominate the recombination process, in order of their contributions to  $\alpha_R(T)$ , for each of the 15 ions considered here at  $\log_{10} T = 2, 3$ , and 4. The resonances of the “high- $n$ ” states do not significantly contribute until  $T \sim 20,000$  K, depending on the ion. This is clear from some of the recombination rates shown in the figures above. Table 2 also presents the percentage contributions of these dominant states to the total rates. A few points may be noted. The number of contributing states that dominate  $\alpha_R(T)$  for an ion is not the same at all temperatures; the number is usually larger at higher temperatures, beyond 10,000 K. The order of contributions of the dominant states is also not the same at different temperatures. The variation in the individual contributions depends on the distribution of the autoionizing resonances in the photoionization cross sections.

As expected, the ground state is the dominant contributor to the total  $\alpha_R(T)$  for most ions, but not for all. The ground states for the ions in this work are:  $2s^2 2p^2 3P$  for the carbon-like ions,  $3s^2 3p^2 3P^o$  for Si I,  $3s^2 3p^2 3P^o$  for Si II,  $3s^2 3p^3 4S^o$  for S II,  $3s^2 3p^2 3P$  for S III, and  $2s^2 2p^2 3P^o$  for C II. In Table 2 the ground state

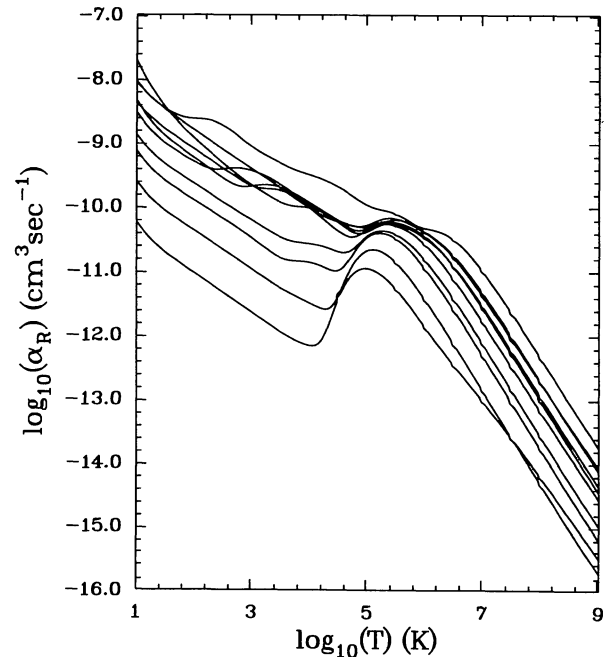


FIG. 3.—Total recombination rate coefficient,  $\alpha_R(T)$ , for the carbon-like ions C I, N II, O III, F IV, Ne V, Na VI, Mg VII, Al VIII, Si IX, and S XI, the lowest curve corresponding to C I. In the low- $T$  region the curves, beyond F IV, overlap because of low- $T$  bumps, but in the high- $T$  region they systematically tend to converge with increment of the ion charge, the topmost curve corresponding to S XI.

TABLE 2  
 RECOMBINATION RATE COEFFICIENTS (in units of  $\text{cm}^3 \text{s}^{-1}$ ) OF THE DOMINANT STATES  
 OF THE IONS<sup>a</sup>

100 (K)			1000 (K)			10,000 (K)		
C I : N <sub>bnd</sub> = 246								
2s22p2		3Pe 2.54-12	2s22p2		3Pe 8.11-13	2s22p2		3Pe 2.82-13
2s22p2		1De 7.73-13	2s22p2		1De 2.50-13	2s22p2		1De 1.64-13
2s22p2	2Po 3d	3Fo 1.51-13	2s22p2	2Po 3d	3Fo 4.55-14	2s2p3		3Do 3.45-14
2s22p2		1Se 1.32-13	2s22p2		1Se 4.20-14	2s22p2		1Se 1.52-14
2s22p2	2Po 3d	3Do 9.16-14	2s22p2	2Po 3d	3Do 2.73-14	2s22p2	2Po 3d	3Fo 1.05-14
2s22p2	2Po 4d	3Fo 8.39-14	2s22p2	2Po 4d	3Fo 2.55-14	2s22p2	2Po 4d	3Fo 6.12-15
2s22p2	2Po 4d	3Do 5.40-14	2s22p2	2Po 4d	3Do 1.62-14	2s22p2	2Po 3d	3Do 6.03-15
2s2p3		1Do 4.71-14	2s2p3		1Do 1.44-14	2s22p2	2Po 3p	3De 5.86-15
2s22p2	2Po 5d	3Fo 4.61-14	2s22p2	2Po 5d	3Fo 1.42-14	2s22p2	2Po 3s	3Po 4.78-15
2s22p2	2Po 4f	3Ge 4.41-14	2s22p2	2Po 3p	3De 1.25-14	2s22p2	2Po 3p	3Pe 4.09-15
2s22p2	2Po 3p	3De 4.09-14	2s22p2	2Po 4f	3Ge 1.21-14	2s22p2	2Po 4d	3Do 3.63-15
2s22p2	2Po 3d	1Fo 4.00-14	2s22p2	2Po 3d	1Fo 1.19-14	2s2p3		1Do 3.50-15
2s22p2	2Po 5f	3Ge 3.91-14	2s22p2	2Po 5f	3Ge 1.08-14	2s22p2	2Po 5d	3Fo 3.47-15
2s22p2	2Po 4f	3Fe 3.62-14	2s22p2	2Po 4f	3Fe 1.00-14			
2s22p2	2Po 5f	3Fe 3.17-14	2s2p3		3Do 9.80-15			
2s22p2	2Po 5d	3Do 3.12-14	2s22p2	2Po 5d	3Do 9.39-15			
2s2p3		3Do 2.92-14	2s22p2	2Po 3s	3Po 8.86-15			
2s22p2	2Po 6f	3Ge 2.84-14	2s22p2	2Po 5f	3Fe 8.76-15			
2s22p2	2Po 3s	3Po 2.79-14	2s22p2	2Po 6d	3Fo 8.46-15			
2s22p2	2Po 6d	3Fo 2.74-14	2s22p2	2Po 6f	3Ge 7.79-15			
Sum: 20 states=		4.29-12	20 states=		1.36-12	13 states=		5.44-13
Total=		9.13-12			2.21-12			6.78-13
%contribution=		47			61			80
N II : N <sub>bnd</sub> = 255								
2s22p2		3Pe 7.62-12	2s22p2		3Pe 2.44-12	2s22p2		3Pe 8.31-13
2s22p2		1De 4.03-12	2s22p2		1De 1.28-12	2s22p2		1De 4.21-13
2s22p2		1Se 8.07-13	2s22p2		1Se 2.55-13	2s2p3		3Do 3.28-13
2s22p2	2Po 3d	3Fo 6.03-13	2s22p2	2Po 3d	3Fo 1.88-13	2s2p3		3Po 1.54-13
2s22p2	2Po 3p	3De 4.04-13	2s22p2	2Po 3p	3De 1.29-13	2s22p2		1Se 8.27-14
2s22p2	2Po 4d	3Fo 3.61-13	2s22p2	2Po 4d	3Fo 1.13-13	2s22p2	2Po 3s	3Po 6.17-14
2s22p2	2Po 3d	3Do 3.52-13	2s22p2	2Po 3d	3Do 1.09-13	2s22p2	2Po 3d	3Fo 5.26-14
2s22p2	2Po 3p	3Pe 2.34-13	2s22p2	2Po 3p	3Pe 7.51-14	2s22p2	2Po 3p	3De 4.84-14
2s22p2	2Po 4d	3Do 2.26-13	2s2p3		3Do 7.25-14	2s22p2	2Po 4f	3Fo 3.26-14
2s2p3		3Do 2.16-13	2s22p2	2Po 3s	3Po 7.07-14	2s22p2	2Po 3d	3Do 2.97-14
2s22p2	2Po 3s	3Po 2.16-13	2s22p2	2Po 4d	3Do 7.04-14	2s22p2	2Po 3p	3Pe 2.87-14
2s22p2	2Po 5d	3Fo 2.01-13	2s22p2	2Po 5d	3Fo 6.32-14	2s2p3		3So 2.24-14
2s22p2	2Po 4f	3Ge 1.82-13	2s22p2	2Po 3d	3Po 5.64-14	2s22p2	2Po 4d	3Do 1.96-14
2s22p2	2Po 3d	3Po 1.82-13	2s22p2	2Po 4f	3Ge 5.54-14	2s22p2	2Po 5d	3Fo 1.86-14
2s22p2	2Po 5f	3Ge 1.62-13	2s22p2	2Po 5f	3Ge 4.92-14	2s22p2	2Po 3p	1De 1.78-14
2s22p2	2Po 3p	1De 1.48-13	2s22p2	2Po 3p	1De 4.73-14	2s22p2	2Po 3d	3Po 1.54-14
2s22p2	2Po 4f	3Fe 1.47-13	2s22p2	2Po 4f	3Fe 4.46-14	2s22p2	2Po 4p	3De 1.31-14
2s22p2	2Po 5d	3Do 1.35-13	2s22p2	2Po 5d	3Do 4.20-14	2s22p2	2Po 4f	3Ge 1.31-14
2s22p2	2Po 3d	1Fo 1.34-13	2s22p2	2Po 3d	1Fo 4.14-14	2s22p2	2Po 5d	3Do 1.18-14
2s22p2	2Po 5f	3Fe 1.29-13	2s22p2	2Po 4d	3Po 3.93-14	2s22p2	2Po 5f	3Ge 1.17-14
Sum: 20 states=		1.65-11	20 states=		5.25-12	20 states=		2.21-12
Total=		4.18-11			1.04-11			3.10-12
%contribution=		40			50			71
O III: N <sub>bnd</sub> = 284								
2s22p2		3Pe 1.52-11	2s22p2		3Pe 6.54-12	2s2p3		3Do 4.10-12
2s2p3		1Po 1.29-11	2s22p2		1De 2.00-12	2s22p2		3Pe 1.56-12
2s22p2	2Po 3s	1Po 7.21-12	2s2p3		1Po 1.74-12	2s2p3		3Po 9.23-13
2s22p2		1De 6.24-12	2s22p2	2Po 3s	1Po 1.11-12	2s22p2		1De 6.60-13
2s2p3		3Do 1.88-12	2s2p3		3Do 6.72-13	2s22p2	2Po 3s	3Po 4.63-13
2s22p2	2Po 3p	3De 1.69-12	2s22p2	2Po 3p	3Se 6.01-13	2s2p3		1Do 4.49-13
2s22p2		1Se 1.59-12	2s22p2	2Po 3p	3De 5.16-13	2s22p2	2Po 3d	3Fo 3.14-13
2s22p2	2Po 3p	3Se 1.38-12	2s22p2		1Se 5.05-13	2s22p2	2Po 3p	3De 2.33-13
2s22p2	2Po 3p	3Pe 1.06-12	2s22p2	2Po 3p	3Pe 3.24-13	2s22p2	2Po 3d	3Do 2.22-13
2s22p2	2Po 3d	3Fo 1.02-12	2s22p2	2Po 3d	3Fo 3.10-13	2s2p3		1Po 1.98-13
2s22p2	2Po 4d	3Fo 8.16-13	2s22p2	2Po 4d	3Fo 2.55-13	2s22p2		1Se 1.74-13
2s22p2	2Po 3d	3Do 6.05-13	2s2p2		4Pe 3d 3De 2.40-13	2s22p2	2Po 3s	1Po 1.63-13
2s22p2	2Po 3s	3Po 5.74-13	2s22p2	2Po 3s	3Po 1.87-13	2s2p3		3So 1.17-13
2s22p2	2Po 3d	3Po 4.74-13	2s22p2	2Po 3d	3Do 1.82-13	2s22p2	2Po 3p	3Pe 1.16-13
2s22p2	2Po 4d	3Do 4.73-13	2s22p2	2Po 4d	3Do 1.48-13	2s2p2	4Pe 3p	3Do 8.06-14

TABLE 2—Continued

O III: Nbnd = 284

2s22p	2Po 5d 3Fo	4.50-13	2s22p	2Po 5p 3Pe	1.48-13	2s22p	2Po 3d 3Po	7.21-14
2s22p	2Po 3d 1Po	4.34-13	2s22p	2Po 3d 3Po	1.47-13	2s22p	2Po 4d 3Fo	7.07-14
2s22p	2Po 4f 3Ge	4.07-13	2s22p	2Po 5d 3Fo	1.41-13	2s2p2	4Pe 3d 3De	6.27-14
2s2p2	4Pe 3d 3De	3.92-13	2s22p	2Po 5p 3De	1.37-13	2s22p	2Po 3d 1Fo	5.84-14
2s22p	2Po 4p 3De	3.81-13	2s22p	2Po 4p 3Pe	1.37-13	2s22p	2Po 3p 3Se	5.83-14
Sum:	20 states=	5.52-11		20 states=	1.60-11		20 states=	1.01-11
Total=		1.24-10			3.15-11			1.33-11
%contribution=		45			51			76

F IV : Nbnd = 324

2s22p2	3Pe	2.00-11	2s22p2	3Pe	6.33-12	2s2p3	3Do	3.82-12
2s2p3	1Po	1.68-11	2s2p3	1Po	4.04-12	2s22p2	3Pe	2.54-12
2s22p2	1De	1.02-11	2s22p2	1De	3.26-12	2s22p	2Po 3d 3Fo	1.91-12
2s22p	2Po 3d 3Fo	7.18-12	2s2p3	3Do	3.06-12	2s2p3	1Do	1.50-12
2s2p3	3Do	6.37-12	2s22p	2Po 3d 3Fo	2.34-12	2s2p3	3Po	1.37-12
2s2p3	3Po	4.36-12	2s2p3	3Po	1.83-12	2s2p3	3So	1.37-12
2s22p	2Po 3d 1Do	4.35-12	2s2p3	1Do	1.27-12	2s22p2	1De	1.19-12
2s2p3	1Do	3.83-12	2s22p	2Po 3d 1Do	1.03-12	2s2p3	1Po	1.18-12
2s22p	2Po 3d 1Po	3.51-12	2s22p	2Po 3d 1Po	8.45-13	2s22p	2Po 3d 3Do	9.72-13
2s22p	2Po 3d 1Fo	3.05-12	2s22p	2Po 3d 1Fo	7.81-13	2s22p	2Po 3d 3Po	4.04-13
2s22p	2Po 3p 3De	2.32-12	2s22p	2Po 3p 3De	7.32-13	2s22p	2Po 3d 1Do	3.37-13
2s22p2	1Se	1.95-12	2s22p	4Pe 3p 3Do	6.42-13	2s2p2	4Pe 3p 3Do	3.36-13
2s22p	2Po 4d 3Fo	1.31-12	2s22p2	1Se	6.21-13	2s22p	2Po 3d 1Fo	3.06-13
2s22p	2Po 3p 3Pe	1.30-12	2s22p	2Po 3p 3Pe	4.14-13	2s22p	2Po 3p 3De	2.39-13
2s22p	2Po 3d 3Po	1.28-12	2s22p	2Po 4d 3Fo	4.12-13	2s2p2	4Pe 3d 3De	2.25-13
2s22p	2Po 3d 3Do	1.20-12	2s22p	2Po 3d 3Po	3.57-13	2s22p2	1Se	2.03-13
2s22p	2Po 3s 3Po	9.01-13	2s22p	2Po 3d 3Do	3.52-13	2s22p	2Po 4s 3Po	1.80-13
2s22p	2Po 3p 1De	8.06-13	2s22p	2Po 3s 3Po	2.81-13	2s22p	2Po 3d 1Po	1.60-13
2s22p	2Po 5d 3Fo	7.93-13	2s2p2	4Pe 4p 3Do	2.77-13	2s22p	2Po 3p 3Pe	1.43-13
2s22p	2Po 5f 3Ge	7.22-13	2s22p	2Po 5d 3Fo	2.50-13	2s2p2	2De 3p 3Fo	1.41-13
Sum:	20 states=	9.22-11		20 states=	2.91-11		20 states=	1.85-11
Total=		2.25-10			6.00-11			2.60-11
%contribution=		41			48			71

Ne V : Nbnd = 338

2s2p3	3Do	1.30-10	2s2p3	3Do	1.51-10	2s2p3	3Do	1.67-11
2s2p3	3Po	2.90-11	2s2p3	3Po	6.90-11	2s2p3	3Po	1.26-11
2s22p2	3Pe	2.58-11	2s2p3	1Do	1.91-11	2s2p3	1Do	7.69-12
2s22p2	1De	1.29-11	2s2p2	2De 3p 3Do	8.64-12	2s2p2	2De 3d 3Fe	4.98-12
2s2p2	2De 3p 3Fo	1.09-11	2s22p2	3Pe	8.17-12	2s2p2	2De 3d 3Ge	4.87-12
2s22p	2Po 4d 3Fo	9.56-12	2s2p2	2De 3p 3Po	7.65-12	2s2p2	4Pe 3d 3Fe	3.87-12
2s22p	2Po 4d 3Do	8.24-12	2s2p2	2De 3p 1Fo	4.88-12	2s2p2	2De 3d 3De	2.89-12
2s2p2	2De 3p 3Do	7.64-12	2s22p	2Po 4d 3Do	4.77-12	2s22p2	3Pe	2.81-12
2s22p	2Po 3d 3Fo	7.41-12	2s22p2	1De	4.07-12	2p4	1De	2.25-12
2s22p	2Po 3d 3Do	4.75-12	2s2p2	2De 3p 3Fo	3.93-12	2s2p2	2De 3d 1Fe	1.73-12
2s22p	2Po 3p 3De	3.76-12	2s22p	2Po 4d 3Fo	2.62-12	2s2p3	1Po	1.71-12
2s22p2	1Se	2.99-12	2s2p2	2De 3d 3Fe	2.46-12	2s2p2	2De 3d 1Ge	1.49-12
2s2p2	2De 3p 3Po	2.56-12				2s2p2	2De 3d 1De	1.45-12
2s2p2	2De 3d 3Ge	2.46-12				2p4	3Pe	1.44-12
2s22p	2Po 3d 3Po	2.23-12				2s22p2	1De	1.39-12
2s22p	2Po 3p 3Pe	2.13-12				2s2p2	2De 3p 3Po	1.34-12
2s2p2	2De 3d 3Fe	2.06-12				2s2p2	2De 3p 1Fo	1.13-12
2s22p	2Po 3d 1Do	1.60-12				2s2p2	2De 3d 1Pe	1.11-12
2s22p	2Po 4p 3De	1.43-12				2s2p2	2De 3d 3Pe	1.04-12
2s2p3	1Do	1.26-12				2s2p2	2De 3p 3Do	8.86-13
Sum:	20 states=	2.69-10		12 states=	2.87-10		20 states=	7.34-11
Total=		4.92-10			3.56-10			9.46-11
%contribution=		55			81			78

Na VI: Nbnd = 390

2s22p2	3Pe	1.24-10	2p4	3Pe	5.05-11	2p4	3Pe	2.91-11
2s22p2	1De	1.72-11	2s22p2	3Pe	3.18-11	2p4	1De	1.44-11
2p4	3Pe	1.05-11	2s2 2p	2Po 4p 3De	9.21-12	2s2p3	3Do	9.12-12
2s 2p2	4Pe 3s 3Pe	8.20-12	2s22p2	1De	5.76-12	2s22p2	3Pe	7.96-12
2s2 2p	2Po 4f 3Ge	6.25-12	2s 2p2	2Pe 3s 3Pe	3.32-12	2s2p3	3Po	5.55-12

TABLE 2—Continued

Na VI: Nband = 390

2s2 2p 2Po 3d 3Fo	6.20-12	2s 2p2 2Pe 3d 3Fe	2.21-12	2s2 2p 2Po 4p 3De	4.31-12
2s2 2p 2Po 3p 3De	5.42-12	2s2 2p 2Po 3d 3Fo	1.95-12	2s22p2	1De 2.01-12
2s22p2	1Se 4.21-12	2s2 2p 2Po 3p 3De	1.70-12	2s 2p2 2Pe 3s 3Pe	1.79-12
2s2 2p 2Po 4f 3De	4.06-12	2s22p2	1Se 1.40-12	2s 2p2 4Pe 3p 3Do	1.25-12
2s2 2p 2Po 3d 3Do	3.74-12	2s2 2p 2Po 4f 3Ge	1.32-12	2s22p2	1Se 1.24-12
2s2 2p 2Po 4p 3Pe	3.45-12	2s2 2p 2Po 4p 3Pe	1.29-12	2s 2p2 2Pe 3d 3Fe	1.09-12
2s2 2p 2Po 4d 3Fo	3.39-12	2s 2p2 2De 3d 3Fe	1.24-12	2s 2p2 4Pe 3p 3Po	9.43-13
2s2 2p 2Po 3p 3Pe	3.30-12	2s2 2p 2Po 4f 3De	1.18-12	2s2 2p 2Po 4p 1De	8.81-13
2s2 2p 2Po 4p 3De	3.05-12	2s2 2p 2Po 3d 3Do	1.18-12	2s 2p2 2De 3d 3Fe	7.66-13
2s 2p2 4Pe 3d 3De	2.67-12	2p4	1De 1.15-12	2s2 2p 2Po 4p 3Pe	7.57-13
2s2 2p 2Po 3d 3Po	2.54-12	2s2 2p 2Po 4d 3Fo	1.07-12	2s 2p2 2De 3d 3De	6.55-13
2p4	1De 2.20-12	2s 2p2 2De 3d 3De	1.06-12	2s 2p2 4Pe 3d 3De	6.18-13
2s2 2p 2Po 4f 3Fe	2.19-12	2s2 2p 2Po 3p 3Pe	9.36-13	2s2 2p 2Po 4d 3Fo	6.06-13
2s2 2p 2Po 3s 3Po	2.13-12	2s2 2p 2Po 5p 3De	8.86-13	2s2 2p 2Po 3d 3Fo	6.04-13
2s 2p2 4Pe 4d 3De	1.99-12	2s 2p2 2Se 3d 3De	8.61-13	2s 2p2 2Se 3d 3De	6.01-13
Sum: 20 states=	2.16-10	20 states=	1.20-10	20 states=	8.43-11
Total=	5.68-10		2.05-10		1.13-10
%contribution=	38		58		75

Mg VII: Nband = 412

2s22p2	1De 2.08-10	2s22p2	1De 2.78-11	2s2p3	3Do 1.57-11
2s2p2 2De 4d 1Ge	7.95-11	2s22p2	3Pe 1.28-11	2s22p2	1De 1.19-11
2s2p2 2De 3d 1Ge	5.31-11	2s2p2 2De 3s 1De	6.50-12	2s22p2	3Pe 4.21-12
2s2p2 2De 3s 1De	4.67-11	2s2p2 2De 4d 1Ge	4.41-12	2s2p3	3Po 4.17-12
2s22p2	3Pe 3.79-11	2s2p2 2De 3s 3De	3.70-12	2s2p2 2De 3p 3Fo	2.75-12
2s2p2 2De 4d 1Fe	2.75-11	2s2p2 2De 3d 1Ge	2.96-12	2s2p2 2De 3d 3Ge	1.73-12
2p4	1De 2.22-11	2s22p 2Po 3d 3Fo	2.52-12	2s2p2 2De 3p 3Do	1.63-12
2s2p2 2De 3d 1Fe	2.12-11	2s22p 2Po 3p 3De	2.38-12	2s2p2 2De 3d 3Fe	1.38-12
2s2p2 2De 3d 1De	1.91-11	2s22p 2Po 3d 3Do	1.67-12	2s2p3	1Do 1.16-12
2s22p 2Po 5p 1De	1.32-11	2s22p 2Po 5p 1De	1.61-12	2s2p2 2De 4f 3Ho	1.13-12
2s2p2 2Se 3d 1De	9.47-12	2s2p2 2De 4d 1Fe	1.52-12	2s2p2 2De 4f 3Go	1.05-12
2s2p2 2De 4s 1De	9.09-12	2s22p 2Po 4d 3Fo	1.50-12	2s2p3	1Po 8.27-13
2s22p 2Po 3p 1De	8.68-12	2s22p2	1Se 1.46-12	2s22p 2Po 3d 3Fo	8.04-13
2s22p 2Po 7f 1Ge	8.54-12	2s22p 2Po 5p 3Se	1.44-12	2s2p2 2De 4p 3Fo	7.68-13
2s22p 2Po 5p 1Pe	8.45-12	2s22p 2Po 5p 3Pe	1.30-12	2s2p2 2De 4d 3Ge	7.26-13
2s22p 2Po 3d 3Fo	8.04-12	2s22p 2Po 3p 3Pe	1.25-12	2s22p 2Po 3p 3De	7.18-13
2s22p 2Po 3p 3De	7.44-12	2p4	1De 1.25-12	2s2p2 2De 3p 3Po	6.82-13
2s22p 2Po 6p 1De	6.63-12	2s22p 2Po 3p 1De	1.22-12	2s2p2 2De 3s 1De	6.77-13
2s22p 2Po 3d 3Do	5.28-12	2s22p 2Po 4d 3Do	1.21-12	2s2p2 2De 3d 3De	6.67-13
2p3 2Do 3p 1De	4.76-12	2s2p2 2De 4s 1De	1.20-12	2s2p2 2De 3s 3De	6.64-13
Sum: 20 states=	6.05-10	20 states=	7.97-11	20 states=	5.33-11
Total=	1.16-9		2.10-10		9.39-11
%contribution=	52		38		57

Al VIII: Nband = 431

2s22p2	3Pe 4.91-11	2s22p2	3Pe 1.58-11	2s2p3	3Do 2.50-11
2s22p2	1De 2.61-11	2s2p3	3Do 8.50-12	2p4	3Pe 1.01-11
2s22p 2Po 3d 3Fo	1.05-11	2s22p2	1De 8.24-12	2s2p3	3Po 7.11-12
2s22p 2Po 3p 3De	9.00-12	2s22p 2Po 3d 3Fo	3.31-12	2s22p2	3Pe 5.09-12
2s22p 2Po 3d 3Do	6.34-12	2s22p 2Po 3p 3De	2.85-12	2s2p2 4Pe 3p 3Do	3.35-12
2s22p 2Po 4d 3Fo	5.62-12	2s22p 2Po 3d 3Do	2.00-12	2s22p2	1De 2.63-12
2s22p2	1Se 5.54-12	2s22p2	1Se 1.83-12	2s2p2 4Pe 3d 3De	2.35-12
2s22p 2Po 3p 3Pe	4.87-12	2s22p 2Po 4d 3Fo	1.79-12	2s2p2 4Pe 4d 3De	1.65-12
2s22p 2Po 3d 3Po	4.28-12	2s22p 2Po 3p 3Pe	1.56-12	2p3	4So 3p 3Pe 1.28-12
2s22p 2Po 3s 3Po	4.02-12	2s22p 2Po 3d 3Po	1.36-12	2s2p2 4Pe 4p 3Do	1.21-12
2s22p 2Po 4d 3Do	4.01-12	2s22p 2Po 3s 3Po	1.27-12	2s2p2 4Pe 3p 3Po	1.04-12
2s22p 2Po 4f 3Ge	3.25-12	2s22p 2Po 4d 3Do	1.26-12	2s22p 2Po 3d 3Fo	1.03-12
2s22p 2Po 5f 3Ge	3.12-12	2s2p2 4Pe 3p 3Do	1.16-12	2s22p 2Po 3p 3De	9.03-13
2s22p 2Po 5d 3Fo	2.88-12	2s2p3	3Po 1.12-12	2s2p2 4Pe 5d 3De	8.34-13
2s22p 2Po 3p 1De	2.70-12	2s22p 2Po 4f 3Ge	1.03-12	2s2p2 4Pe 4d 3Fe	7.92-13
2s22p 2Po 4d 3Po	2.62-12	2s22p 2Po 5f 3Ge	9.76-13	2s2p2 4Pe 3d 3Fe	7.56-13
2s22p 2Po 3d 1Do	2.59-12	2s22p 2Po 5d 3Fo	9.13-13	2s22p 2Po 3d 3Do	6.30-13
2s22p 2Po 4f 3Pe	2.20-12	2s22p 2Po 3p 1De	8.56-13	2s2p2 4Pe 4f 3Fo	6.03-13
2s22p 2Po 3d 1Fo	2.07-12	2s22p 2Po 4d 3Po	8.24-13	2s22p2	1Se 5.85-13
2s22p 2Po 4p 3Pe	2.06-12	2s22p 2Po 3d 1Do	8.22-13	2s2p2 4Pe 5p 3Do	5.66-13
Sum: 20 states=	1.53-10	20 states=	5.74-11	20 states=	6.75-11
Total=	7.80-10		2.05-10		1.06-10
%contribution=	20		28		64



TABLE 2—Continued

Si IX : N<sub>bnd</sub> = 450

2p4	1De	9.75-10	2p4	1De	3.79-10	2p4	3Pe	6.16-11
2p3	2Do	3p 1Pe	2p3	2Do	3p 1Pe	2p4	1De	2.96-11
2s22p2		3Pe	2p4		3Pe	2p3	2Do	3d 3Go
2s22p2		1De	2s22p2		3Pe	2p3	2Do	3d 3Fo
2p3	2Do	3p 1De	2s22p2		1De	2s22p2		3Pe
2p4		3Pe	2p3	2Do	3p 1De	2p3	2Do	3d 3Do
2p3	2Po	3p 1De	2p3	2Po	3p 1De	2p3	2Do	3d 1Go
2s22p	2Po	3d 3Fo	2s22p2		1Se	2s22p2		1De
2s2p2	2De	4d 1De	2p3	2Do	3p 3Pe	2p3	2Do	3p 3Pe
2s22p	2Po	3p 3De	2s2p2	2De	4d 1De	2s2p3		3Po
2s22p2		1Se	2s22p	2Po	5p 3De	2s22p2		1Se
2s2p2	2Pe	3s 1Pe	2s2p2	2Pe	3s 3Pe	2s2p3		3Do
2s22p	2Po	5p 1De	2s22p	2Po	3d 3Fo	2s22p	2Po	5p 3De
2s22p	2Po	3d 3Do	2s22p	2Po	3p 3De	2p3	2Do	3d 1Fo
2s22p	2Po	4d 3Fo	2s2p2	2Pe	3s 1Pe	2p3	2Do	3p 1Pe
2s22p	2Po	5p 3De	2s22p	2Po	5p 1De	2s2p2	2Pe	3s 3Pe
2s22p	2Po	3p 3Pe	2s22p	2Po	3d 3Do	2p3	2Do	3p 3De
2s2p2	2Pe	4d 1Pe	2s2p2	2Pe	4d 1Pe	2p3	2Po	3p 3De
2s2p2	2De	4d 1Se	2p3	2Do	3p 3De	2s2p2	2Pe	4s 3Pe
2s22p	2Po	3d 3Po	2s22p	2Po	4d 3Fo	2p3	4So	3d 3Do
Sum:	20 states=	1.44-9	20 states=	6.14-10	20 states=	2.10-10		
Total=		2.34-9		8.44-10		3.07-10		
%contribution=		62		73		69		

S XI : N<sub>bnd</sub> = 498

2s22p2	3Pe	8.17-11	2s22p2	3Pe	2.44-11	2s22p2	3Pe	7.99-12
2s22p2		1De	2s22p2		1De	2s22p2		1De
2s22p	2Po	3d 3Fo	2s22p	2Po	3d 3Fo	2s22p	2Po	3d 3Fo
2s22p	2Po	3p 3De	2s22p	2Po	3p 3De	2s22p	2Po	3p 3De
2s22p	2Po	3d 3Do	2s22p	2Po	3d 3Do	2s22p	2Po	3d 3Do
2s22p	2Po	4d 3Fo	2s22p	2Po	4d 3Fo	2s22p	2Po	4d 3Fo
2s22p2		1Se	2s22p2		1Se	2s22p2		1Se
2s22p	2Po	3p 3Pe	2s22p	2Po	3p 3Pe	2s22p	2Po	3p 3Pe
2s22p	2Po	3s 3Po	2s22p	2Po	3s 3Po	2s22p	2Po	3s 3Po
2s22p	2Po	3d 3Po	2s22p	2Po	3d 3Po	2s22p	2Po	3d 3Po
2s22p	2Po	4p 3De	2s22p	2Po	4p 3De	2s22p	2Po	4p 3De
2s22p	2Po	4d 3Do	2s22p	2Po	4d 3Do	2s22p	2Po	4d 3Do
2s22p	2Po	4f 3Ge	2s22p	2Po	4f 3Ge	2s22p	2Po	4f 3Ge
2s22p	2Po	5f 3Ge	2s22p	2Po	5f 3Ge	2s22p	2Po	5f 3Ge
2s22p	2Po	3p 1De	2s22p	2Po	3p 1De	2s22p	2Po	5f 3Ge
2s22p	2Po	4f 3Fe	2s22p	2Po	4f 3Fe	2s22p	2Po	4f 3Fe
2s22p	2Po	5f 3Fe	2s22p	2Po	5f 3Fe	2s22p	2Po	5f 3Fe
2s22p	2Po	4d 3Po	2s22p	2Po	3d 1Do	2s22p	2Po	3d 1Do
2s22p	2Po	3d 1Do	2s22p	2Po	4d 3Po	2s22p	2Po	4d 3Po
2s22p	2Po	3d 1Fo	2s22p	2Po	4p 3Pe	2s22p	2Po	4p 3Pe
Sum:	20 states=	2.61-10	20 states=	8.18-11	20 states=	2.62-11		
Total=		1.56-9		3.79-10		9.31-11		
%contribution=		17		22		28		

Si I : N<sub>bnd</sub> = 264

3s23p2	3Pe	4.74-12	3s23p2	3Pe	1.51-12	3s23p2	3Pe	4.73-13
3s23p2		1De	3s23p2		1De	3s23p2		1De
3s23p	2Po	4p 3De	3s23p	2Po	4p 3De	3s3p2	4Pe	3d 3De
3s23p	2Po	3d 3Fo	3s23p	2Po	3d 3Fo	3s3p2	4Pe	4f 3Go
3s23p	2Po	4p 3Pe	3s23p	2Po	4p 3Pe	3s3p2	2De	4f 3Ho
3s3p3		3Do	3s3p3		3Do	3p4		3Pe
3s23p	2Po	5p 3Pe	3s23p	2Po	5p 3Pe	3s23p	2Po	3d 3Fo
3s23p	2Po	5p 3De	3s23p	2Po	4p 1De	3s3p3		3Do
3s23p	2Po	4p 1De	3s23p	2Po	5p 3De	3s3p2	4Pe	4f 3Fo
3s23p	2Po	3d 3Po	3s23p	2Po	3d 1Do	3s23p	2Po	4p 3De
3s23p2		1Se	3s23p	2Po	3d 3Po	3s3p2	2De	3d 1Pe
3s23p	2Po	3d 1Do	3s23p2		1Se	3s23p	2Po	5p 3Pe
3s23p	2Po	4d 3Fo	3p4		3Pe	3s23p	2Po	4p 3Pe
3p4		3Pe	3s23p	2Po	4d 3Fo	3s3p2	2De	4f 1Go
3s23p	2Po	5p 1De	3s23p	2Po	5p 1De	3p4		1De
3s23p	2Po	6h 3Te	3s3p2	4Pe	3d 3De	3s23p	2Po	5p 3De
3s3p2	4Pe	3d 3De	3s23p	2Po	6h 3Te	3s3p2	2De	4f 1Ho
3s23p	2Po	7h 3Te	3s23p	2Po	7h 3Te	3s23p	2Po	4d 3Do
3s23p	2Po	4p 1Pe	3s23p	2Po	5p 3Se	3s3p2	2De	3d 3Se

TABLE 2—Continued

Si I : Nband = 264

3s23p	2Po 6h 3He	4.92-14	3s23p	2Po 6h 3He	1.45-14	3s23p2	1Se	1.33-14
Sum:	20 states=	8.28-12		20 states=	2.65-12		20 states=	1.18-12
Total=		1.36-11			3.72-12			1.60-12
%contribution=		61			71			74

Si II: Nband = 59

3s3p2	2De	3.46-12	3s3p2	2De	1.08-12	3s2	1Se 3d 2De	5.28-13
3p3	2Po	1.59-12	3p3	2Po	4.58-13	3s3p2		2De 4.56-13
3s2	1Se 4d 2De	7.41-13	3s2	1Se 4d 2De	2.26-13	3s2	1Se 4s 2Se	2.94-13
3s2	1Se 4f 2Fo	6.42-13	3s2	1Se 4f 2Fo	1.95-13	3p3		2Po 1.88-13
3s2	1Se 5f 2Fo	6.19-13	3s2	1Se 5f 2Fo	1.89-13	3s3p2		2Pe 1.23-13
3s2	1Se 5d 2De	5.07-13	3s2	1Se 5d 2De	1.58-13	3s3p2		2Se 1.13-13
3s2	1Se 6f 2Fo	4.57-13	3s2	1Se 6f 2Fo	1.40-13	3s2	1Se 4p 2Po	8.58-14
3s2	1Se 4p 2Po	4.01-13	3s2	1Se 4p 2Po	1.19-13	3s2	1Se 4d 2De	6.59-14
3s2	1Se 7f 2Fo	3.26-13	3s2	1Se 7f 2Fo	1.00-13	3s3p	3Po 4s 2Po	4.96-14
3s2	1Se 6g 2Ge	3.19-13	3s2	1Se 6d 2De	9.55-14	3s2	1Se 4f 2Fo	4.67-14
3s2	1Se 6d 2De	3.03-13	3s2	1Se 6g 2Ge	9.40-14	3s2	1Se 5f 2Fo	4.48-14
3s2	1Se 7g 2Ge	2.82-13	3s2	1Se 7p 2Po	8.46-14	3s3p	3Po 3d 2Do	4.40-14
3s2	1Se 5p 2Po	2.73-13	3s2	1Se 7g 2Ge	8.32-14	3s2	1Se 5d 2De	4.33-14
3s2	1Se 5g 2Ge	2.72-13	3s2	1Se 5p 2Po	8.26-14	3s2	1Se 6f 2Fo	3.41-14
3s2	1Se 8f 2Fo	2.36-13	3s2	1Se 5g 2Ge	7.98-14	3s2	1Se 7p 2Po	3.38-14
3s2	1Se 8g 2Ge	2.31-13	3s2	1Se 8f 2Fo	7.28-14	3s2	1Se 6d 2De	2.71-14
3s2	1Se 7p 2Po	2.19-13	3s2	1Se 8g 2Ge	6.82-14	3s2	1Se 7f 2Fo	2.47-14
3s2	1Se 6p 2Po	2.01-13	3s2	1Se 6p 2Po	6.37-14	3s2	1Se 5p 2Po	1.97-14
3s2	1Se 7d 2De	1.88-13	3s2	1Se 7d 2De	5.97-14	3s2	1Se 6g 2Ge	1.92-14
3s2	1Se 8h 2Ho	1.87-13	3s2	1Se 9g 2Ge	5.48-14	3s2	1Se 8f 2Fo	1.80-14
Sum:	20 states=	1.15-11		20 states=	3.50-12		20 states=	2.26-12
Total=		3.28-11			7.46-12			2.92-12
%contribution=		35			47			77

S II : Nband = 313

3s23p3	2Po	2.51-12	3s23p3	2Do	1.93-12	3s3p4	4Pe	6.08-13
3s23p3	2Do	1.74-12	3s23p3	2Po	1.06-12	3s23p3		2Do 4.85-13
3s23p2 3Pe 3d 4Fe		1.72-12	3s23p2 3Pe 3d 4Fe		5.05-13	3s23p3		2Po 3.42-13
3s23p3	4So	1.15-12	3s23p2 3Pe 3d 4De		4.34-13	3s23p2 3Pe 3d 4Fe		2.01-13
3s23p2 3Pe 3d 4De		8.18-13	3s23p3	4So	3.25-13	3s23p3		4So 1.32-13
3s23p2 3Pe 3d 2Pe		6.25-13	3s3p4	4Pe	1.97-13	3s23p2 3Pe 3d 4De		1.26-13
3s3p4	4Pe	4.56-13	3s23p2 3Pe 3d 2Pe		1.39-13	3s3p4		2De 1.05-13
3s23p2 3Pe 3d 2Fe		3.72-13	3s23p2 3Pe 3d 2Fe		1.34-13	3s23p2 3Pe 3d 2Fe		6.08-14
3s3p4	2De	3.07-13	3s23p2 3Pe 4d 4Fe		9.69-14	3s23p2 3Pe 3d 2Pe		4.38-14
3s23p2 3Pe 4d 4Fe		2.97-13	3s3p4	2De	8.28-14	3s23p2 1De 4p 2Fo		3.75-14
3s23p2 3Pe 4d 4De		2.16-13	3s23p2 3Pe 3d 4Pe		6.43-14	3s23p2 3Pe 4s 4Pe		3.46-14
3s23p2 3Pe 3d 4Pe		2.09-13	3s23p2 3Pe 4f 4Go		6.36-14	3s23p2 3Pe 4d 4Fe		3.23-14
3s23p2 3Pe 4f 4Go		2.09-13	3s23p2 3Pe 4d 4De		6.21-14	3s23p2 1De 5p 2Fo		2.53-14
3s23p2 3Pe 5f 4Go		1.84-13	3s23p2 1De 4p 2Do		5.97-14	3s23p2 3Pe 4d 4De		2.19-14
3s23p2 3Pe 3d 2De		1.68-13	3s23p2 3Pe 5f 4Go		5.63-14	3s23p2 3Pe 3d 4Pe		2.07-14
3s23p2 3Pe 4p 4Do		1.67-13	3s23p2 3Pe 4s 4Pe		5.31-14	3s23p2 1De 6p 2Fo		1.63-14
3s23p2 3Pe 4d 4Pe		1.54-13	3s23p2 3Pe 4p 4Do		5.20-14	3s23p2 3Pe 4p 4Do		1.61-14
3s23p2 3Pe 4d 2Fe		1.44-13	3s23p2 3Pe 3d 2De		5.17-14	3s23p2 3Pe 4f 4Go		1.51-14
3s23p2 3Pe 4p 2Do		1.43-13	3s23p2 3Pe 4d 4Pe		4.84-14	3s23p2 1De 3d 2Fe		1.49-14
3s23p2 3Pe 4s 4Pe		1.40-13	3s23p2 3Pe 4p 2Do		4.65-14	3s23p2 3Pe 3d 2De		1.47-14
Sum:	20 states=	1.17-11		20 states=	5.46-12		20 states=	2.35-12
Total=		3.80-11			1.11-11			3.40-12
%contribution=		31			49			69

S III: Nband = 309

3s23p	2Po 3d 3Po	6.39-11	3s23p	2Po 3d 3Po	1.09-11	3s23p	2Po 3d 3Do	2.67-12
3s23p	2Po 4s 3Po	2.52-11	3s23p	2Po 3d 3Fo	4.71-12	3s23p	2Po 3d 3Fo	1.84-12
3s3p3	3So	2.49-11	3s3p3	3So	4.52-12	3s23p	2Po 3d 3Po	1.63-12
3s23p	2Po 3d 3Fo	1.46-11	3s23p	2Po 4s 3Po	4.26-12	3s3p3		3So 1.36-12
3s3p3	1Po	6.90-12	3s23p	2Po 3d 1Do	2.52-12	3s23p	2Po 3d 1Do	1.11-12
3s23p	2Po 3d 1Do	6.61-12	3s3p3	1Po	2.43-12	3s23p	2Po 4s 3Po	9.46-13
3s3p3	3Do	6.22-12	3s3p3	3Po	1.54-12	3s23p	2Po 3d 1Po	8.96-13
3s3p3	3Po	4.89-12	3s23p	2Po 4s 1Po	1.42-12	3s3p3		3Po 7.14-13
3s3p3	1Do	4.06-12	3s3p3	1Do	1.40-12	3s3p3		1Po 5.64-13

TABLE 2—Continued

S III: N <sub>bnd</sub> = 309												
3s23p	2Po	3d	1Fo	3.02-12	3s3p3		3Do	1.19-12	3s3p2	4Pe 3d 3Fe 5.55-13		
3s23p	2Po	4s	1Po	2.68-12	3s23p	2Po	3d	1Fo	1.15-12	3s23p	2Po 4s 1Po 5.34-13	
3s3p2	4Pe	3d	5Fe	2.44-12	3s3p2	4Pe	3d	5Fe	7.69-13	3s3p2	2De 3d 3Fe 4.46-13	
3s3p3		5So		1.23-12	3s3p3		5So	3.90-13	3s3p3		3Do 3.79-13	
3s23p	2Po	4d	3Fo	1.01-12	3s23p	2Po	3d	3Do	3.71-13	3s3p3		1Do 3.29-13
3s23p	2Po	4d	3Do	9.40-13	3s23p	2Po	4d	3Fo	3.18-13	3s23p	2Po	4p 3De 3.06-13
3s23p	2Po	3d	3Do	8.44-13	3s23p	2Po	4d	3Do	2.55-13	3s3p2	4Pe	3d 5Fe 2.34-13
3s23p	2Po	4f	3Ge	6.77-13	3s23p	2Po	4f	3Ge	2.12-13	3s23p	2Po	4p 3Pe 1.50-13
3s23p	2Po	4d	3Po	5.84-13	3s3p2	4Pe	4p	3Po	1.97-13	3s23p	2Po	3d 1Po 1.38-13
3s23p	2Po	5d	3Do	5.14-13	3s23p	2Po	4d	3Po	1.69-13			
3s23p2		3Pe		4.90-13	3s23p	2Po	5d	3Do	1.69-13			
Sum:	20 states=			1.72-10		20 states=			3.89-11		18 states=	1.48-11
Total=				2.34-10					5.23-11			1.83-11
%contribution=				73					74			81
C II : N <sub>bnd</sub> = 60												
2p3			2Po	1.13-11	2p3		2Po	3.62-12	2s2p2		2De	2.47-12
2s2	1Se	3d	2De	1.36-12	2s2p2		2De	1.08-12	2p3		2Po	1.24-12
2s2	1Se	2p	2Po	1.29-12	2s2	1Se	3d	2De	4.20-13	2s2	1Se	2p 2Po 1.41-13
2s2p2			2De	9.85-13	2s2	1Se	2p	2Po	4.08-13	2s2	1Se	3d 2De 1.21-13
2s2	1Se	4d	2De	8.46-13	2s2	1Se	4d	2De	2.62-13	2s2	1Se	4d 2De 7.41-14
2s2	1Se	4f	2Fo	5.66-13	2s2	1Se	4f	2Fo	1.72-13	2s2p2		2Se 6.86-14
2s2	1Se	5d	2De	5.24-13	2s2	1Se	5d	2De	1.63-13	2s2	1Se	3s 2Se 6.63-14
2s2	1Se	5f	2Fo	5.11-13	2s2	1Se	5f	2Fo	1.55-13			
2s2	1Se	6f	2Fo	3.81-13	2s2	1Se	3p	2Po	1.16-13			
2s2	1Se	3p	2Po	3.66-13	2s2	1Se	6f	2Fo	1.16-13			
2s2	1Se	6d	2De	3.32-13	2s2	1Se	6d	2De	1.04-13			
2s2	1Se	6g	2Ge	3.03-13	2s2	1Se	6g	2Ge	8.92-14			
2s2	1Se	7f	2Fo	2.78-13	2s2	1Se	7f	2Fo	8.46-14			
2s2	1Se	7g	2Ge	2.67-13	2s2	1Se	3s	2Se	7.95-14			
2s2	1Se	5g	2Ge	2.64-13	2s2	1Se	7g	2Ge	7.86-14			
2s2	1Se	3s	2Se	2.47-13	2s2	1Se	5g	2Ge	7.74-14			
2s2	1Se	8g	2Ge	2.19-13	2s2	1Se	7d	2De	6.52-14			
2s2	1Se	7d	2De	2.07-13	2s2	1Se	8g	2Ge	6.44-14			
2s2	1Se	8f	2Fo	2.05-13	2s2	1Se	8f	2Fo	6.25-14			
2s2	1Se	8h	2Ho	1.84-13	2s2	1Se	4p	2Po	5.85-14			
Sum:	20 states=			2.07-11		20 states=			7.28-12		7 states=	4.18-12
Total=				4.24-11					1.13-11			5.18-12
%contribution=				49					64			81

<sup>a</sup> Given in order of their contributions at temperatures  $\log T = 2, 3, 4$  K.  $N_{bnd}$  corresponds to the total number of low- $n$  bound states for which the detailed photoionization cross sections have been calculated for the total rates. Sum and percentage contribution of these states to the total rates are given at the end of each column.

$2s^2 2p^2 3P$  is the predominant contributor for some of the carbon-like ions, such as C I and N II, but not for some other ions in the sequence, such as Mg VII. The same is true for other ions, e.g., S III ground state,  $3s^2 3p^2 3P$ , is not dominant at some temperatures, but some excited states are. The other important contributors to the total  $\alpha_R(T)$  are the excited equivalent electron states, such as  $2s^2 2p^2 1D$  and  $2p^4 3P$  in carbon-like ions. Although there are only a few, they provide significant contributions to  $\alpha_R(T)$  because of extensive autoionizing resonances in their photoionization cross sections *below* the ionization threshold of the optical electron, as discussed in NP1 and NP2.

Some additional explanation is necessary regarding the uncertainties in the recombination rates for individual states. These rates include the contributions from the low- $n$  ( $n \leq 10$ ) DR-type resonances, as well as the background RR, but not from the high- $n$  ( $n > 10$ ) DR resonances; this effect, however,

is expected to be small at low temperatures up to about 10,000 K for low-charge ions and somewhat higher for highly charged ones. There may be some uncertainties at higher temperatures, since resonances belonging to higher target thresholds, which are not included in the coupled target eigenfunction expansion, are not present in the photoionization cross sections. This should not affect the rates significantly, since comparison of recombination rates obtained using eight state and 23 state calculations for the carbon-sequence ions reveals that additional states in the eigenfunction expansion increase the DR contributions from the higher  $\Delta n \neq 0$  thresholds only slightly. The other source of uncertainty at very high temperatures may arise from inner-shell ionization. Inclusion of some inner-shell ionization by Jacobs et al. (1979) was found to make a negligible contribution to the rate coefficients for Mg and S ions. For these reasons, individual recombination rate coefficients are

given only for  $T = 100, 1000, \text{ and } 10,000 \text{ K}$  in Table 2. Another point regarding Table 2 is the proper identification level for the theoretically calculated bound states. Although great care is taken in their identification, using effective quantum numbers and channel contributions, identification was difficult for some of the states of Si I, and some of the identifications may not be precise.

The recombination rate coefficients of all individual low- $n$  bound states, and the high- $n$  contributions to the

total rate coefficients, may be obtained electronically from [nahar@payne.mps.ohio-state.edu](mailto:nahar@payne.mps.ohio-state.edu).

The author would like to thank Professor Anil K. Pradhan for suggestions and comments. Comments of G. Ferland and D. Verner are thankfully acknowledged. This work was supported by NASA grants NAGW-3315 and NAS-32643. The calculations were performed on the Cray Y-MP at the Ohio Supercomputer Center in Columbus, Ohio.

## REFERENCES

- Aldrovandi, S. M. W., & Péquignot, D. 1973, *A&A*, 25, 137  
 Bell, R. H., & Seaton, M. J. 1985, *J. Phys. B*, 18, 1589  
 Berrington, K. A., Burke, P. G., Butler, K., Seaton, M. J., Storey, P. J., Taylor, K. T., & Yan, Y. 1987, *J. Phys. B*, 20, 6379  
 Jacobs, V. L., Davies, J., & Rogerson, J. E. 1978, *J. Quant. Spectrosc. Radiat. Transfer*, 19, 591  
 Jacobs, V. L., Davies, J., Rogerson, J. E., & Blaha, M. 1979, *ApJ*, 230, 627  
 Liu, X.-W., Storey, P. J., Barlow, M. J., & Clegg, R. E. S. 1965, *MNRAS*, 272, 369  
 Nahar, S. N., & Pradhan, A. K. 1992a, *Phys. Rev. A*, 45, 7887  
 Nahar, S. N., & Pradhan, A. K. 1992b, *ApJ*, 397, 729 (NP3)  
 ———. 1993, *J. Phys. B*, 26, 1109  
 ———. 1994, *Phys. Rev. A*, 49, 1816 (NP1)  
 ———. 1995, *ApJ*, 447, 966 (NP2)  
 Nussbaumer, H., & Storey, P. J. 1983, *A&A*, 126, 75  
 Pradhan, A. K., & Seaton, M. J. 1985, *J. Phys. B*, 18, 1631  
 Seaton, M. J. 1987, *J. Phys. B*, 20, 6363  
 Shull, J. M., & Van Steenberg, M. 1982, *ApJ*, 48, 95  
 Spitzer, L., Jr., & Fitzpatrick, E. L. 1993, *ApJ*, 409, 299